Experimental determinations of the aerodynamic drag for vehicles subjected to the ground effect

Ioan SEBESAN*,[1], Bogdan TARUS[2]

*Corresponding author
*,[1] "POLITEHNICA" University of Bucharest,
Splaiul Independenței 313, 060042, Bucharest, Romania
ioan_sebesan@yahoo.com
[2]Ministry of National Defence, Bucharest, Romania
Izvor Street 110, sector 5, cod 050561
bogtar@gmail.com

DOI: 10.13111/2066-8201.2012.4.2.11

Abstract: *A moving vehicle creates a flow of the surrounding air, continuous and compressible fluid. When the movement is at a constant speed, the air flow is not time dependent and the flow distribution lines are constant. In fact, however, a vehicle moves in an environment where the air itself is in a continuous motion. In addition, there are many side obstacles, such as passing objects, stationary vehicles, artwork, etc. All these factors affect the air flow along the vehicle. The shape and speed of the current lines are affected as compared with time. Based on these considerations, the aerodynamics of any ground vehicle is a non-stationary process. The study of non-stationary phenomena may be related to a steady state study using finite difference method, in which time is divided into finite intervals Δt, small enough so that during a specific period a phenomenon may be considered as stationary. If speeds involved are in subsonic regime, solving the equations of motion is simplified. We may consider therefore that the vehicle is moving at speed V_1 in the air mass at rest, or both, the vehicle is at rest in a stream of air at speed V_1 (this is the particular case of the wind tunnels). For speeds of up to Mach 0.5, the effect of compressibility of air does not influence at all or has very little influence on a flow. In this case, the air density may be considered constant. Also, the effect of viscosity can be neglected in most of the space occupied by the fluid. In order to illustrate the influence of the aerodynamic drag on a ground-effect vehicle we performed a test in the subsonic wind tunnel of the INCAS.*

Key Words: *aerodynamics, vehicles, aerodynamic drag, non-stationary process*

1. INTRODUCTION

In order to express the air flow (velocity field) through a specific equation it must be borne in mind that in every point in space where air flows, there is a velocity vector and the phenomenon may be represented at any time by a vector field $\vec{v}$.

Simplifying assumptions may lead to the fact that this vector field is derived from a scalar potential, denoted φ.

This term is related to the concepts of *flow line* and *stream tube*.

Thus, the flow over surface element *dS* is equal to the volume of a cylinder with its base the generator is the speed vector.

The flow is the volume that flows through *dS* during a time unit (fig.1). If an ideal fluid - incompressible, the quantity is constant.

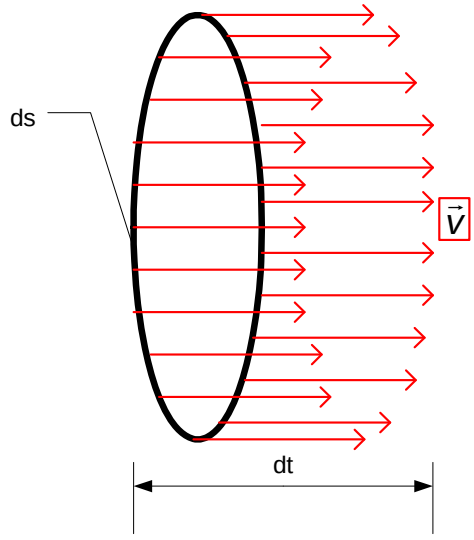

Fig. 1 The air flow along a surface element.

The flow line (fig.2) is a curve tangent to the to the speed vector lines. The flow tube is the closed contour formed by the totality of the flow lines. It is basically a channel that guides the fluid flow.

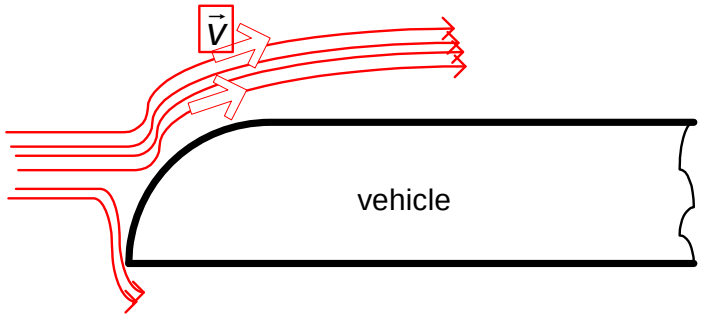

Fig. 2 Flow lines

All the experiments that aim to determine the aerodynamic drag for a vehicle are performed in wind tunnels.

The main element in a wind tunnel is the experimental tunnel.

The fluid must flow through the tunnel with the desired speed, evenly throughout the whole section, in order to assure a correct simulation of the motion of the moving objects in open air.

This result can be achieved, only if the effect of the lateral walls is negligible. In the aerodynamic circuit we have: the *settling chamber*, situated at the start of the circuit which has the role of cancelling all the turbulences in the moving air and to even the speeds of the air currents at the entrance in the tunnel; the *contraction chamber* which accelerates the laminar flow of the air mass coming from the settling room - parallel vectors of speed, with the same direction and equal intensity.

The *wind tunnel* is the room where the replicas are placed and which can have a mobile ceiling in order to achieve variations of the section; the *diffuser*, formed by two subsections: a *divergent nozzle* which reduces the speed of the air flow coming from the experimental

tunnel and the *fan section* which sucks the air out of the tunnel to avoid vortex formations, the *return circuit ,* made of the exact walls of the room in which the wind tunnel is built – at the right angles, deflective screens are placed to duly direct the fluid towards the settling chamber.

2. THE THEORETICAL ANALYSIS OF FLUID DYNAMIC PROCESSES IN WIND TUNNELS

By admitting the fact that such experimental circuit is sufficiently isolated, so the caloric losses which occur through the walls can be negligible, we can consider that the total energy of the weight rate flowing in each section is constant.

Considering V_m, p_m, ρ_m şi T_m the average values of speed, density pressure and temperature, the following equations can be achieved:

$$m = \int_\sigma \rho V d\sigma = \rho_m V_m \sigma$$
$$\frac{1}{2} m V_m^2 = \frac{1}{2} \int_\sigma V^2 \rho V d\sigma \tag{1}$$
$$m T_m = \int_\sigma T \rho V d\sigma$$

where σ is the section and m represents the weight flow.

In the case of a perfectly compressible fluid [2], the energy equation is:

$$\frac{p}{\rho} + c_v T + \frac{1}{2} V^2 = c_p T + \frac{1}{2} V^2 = h + \frac{1}{2} V^2 = c_p T_0 \tag{2}$$

where T_0 is the absolute temperature in points of null speed; h is the enthalpy and c_p is the specific heat at a constant pressure.

By correlating equations (1) and (2) the following results:

$$\frac{p_m}{\rho_m} + c_v T_m + \frac{1}{2} V_m^2 = \frac{\kappa}{\kappa - 1} \cdot \frac{p_m}{\rho_m} + \frac{1}{2} V_m^2 = const. \tag{3}$$

where $\kappa = c_p / c_v$.

In the settling chamber, the fluid (the air) is characterized by the following parameters: p_1 – the pressure; ρ_1 – the density; T_1 – the temperature and v_1 – the speed. By taking into consideration that the speed is very low, the square of this one can be negligible:

$$\frac{\kappa}{\kappa - 1} \frac{p_0}{\rho_0} = \frac{\kappa}{\kappa - 1} \cdot \frac{p_1}{\rho_1} + \frac{1}{2} V^2 \cong \frac{\kappa}{\kappa - 1} \cdot \frac{p_1}{\rho_1} \tag{4}$$

The air mass in the wind tunnel is driven by the fan. The speed of the formed air current depends on the section of the wind tunnel in the measuring point. The maximum value of speed is achieved in the wind tunnel because this is the smallest section of a wind tunnel. But the speed depends also on the power of the fan. Thus, for the maximum value of the power of the fan, normally, the maximum speeds in all the sections of the wind tunnel will be achieved. In all cases, these will be subsonic (in subsonic wind tunnels).

To study the air flow from a thermodynamically view, there must be taken into account the mechanisms of transformations which a moving fluid mass undergoes.

The pressure difference performed by the fan exceeds all the losses of charge from the system caused by frictions, turbulences, vortexes, etc. The fluid mass receives energy from the fan and transfers it to the environment under the form of heat.

The main problem is to determine speed, pressure, density and temperature within the circuit, as well the necessary power to achieve the desired speed in the wind tunnel.

According to Crocco's reasoning, Bernoulli's differential equation can be replaced by the following equation:

$$\eta V dV + \frac{dp}{p} = 0 \tag{5}$$

The differential equation of energy is:

$$c_p dT + V dV = 0 \tag{6}$$

where V is the speed and c_p is the specific heat at a constant pressure.

From equation (6)it results:

$$-VdV = c_p dT = \frac{\kappa}{\kappa - 1} d\left(\frac{p}{\rho}\right) \tag{7}$$

From equation (5) it results:

$$\frac{dp}{p} = -\eta V dV = \eta \frac{\kappa}{\kappa - 1} d\left(\frac{p}{\rho}\right) \tag{8}$$

where η – part of the fluid momentum which turns into potential energy (pressure).

For an average value of η and by integrating equation (8) it is achieved:

$$\frac{\rho}{\rho_0^{'}} = \left(\frac{p}{p_0^{'}}\right)^{1-\frac{\kappa-1}{\kappa}} \tag{9}$$

where ρ_0 and p_0 are the density and pressure in surety for the null speed.

For a polytrophic transformation, p/ρ^n=const. In this case, it is achieved:

$$\frac{1}{n} = 1 - \frac{\kappa - 1}{\kappa} \tag{10}$$

Considering the fact that p/ρ^n=const and η sufficiently low, by integrating the equation it is achieved the equation of speed:

$$V^2 = \frac{2\kappa}{\kappa - 1} \cdot \frac{p_0'}{\rho_0'} \cdot \left[1 - \left(\frac{p}{p_0'}\right)^{\frac{\kappa-1}{\eta\kappa}}\right] \tag{11}$$

Based on experiments, there has been determined that $\eta = 0.67 + 0.12\delta - 0.02\delta^2$, where 2δ is the aperture angle of the diffuser. Usually, the angle measures 6°, for a number of Ma=0, 3÷0, 85 (subsonic state).

Besides the maximum flowing speed of the air in the wind tunnel, the constructional differences between wind tunnels may be:

- The way the wind tunnel is built (closed or opened);
- The movement / no movement of the ground below the replica.
- The suction / no suction of the air flow at ground level.

The Reynold number governs each law of similarity between a full size vehicle and its replica. This is a function that depends on the multiplication of the speed of flowing with the characteristic length of the replica, divided to the kinematic viscosity.

The more the replica is on a close sale to the original vehicle and the more the degree of exterior finishing is similar, the easier is to achieve an adequate Reynolds number between the replica and the 1:1 model.

For ground vehicles, the replicas are used at a 1:7 scale because this allows an acceptable compromise with reality, considering that the wind tunnels used in this domain have no more that 10 m in length [4].

One of the real issues that occur in experiments in wind tunnels is the so-called „air cushion limit" that appears on the lower side of the replica (fig.3).

For example, when a train runs on the tracks, the relative air speed/ground air speed ratio is approximately null.

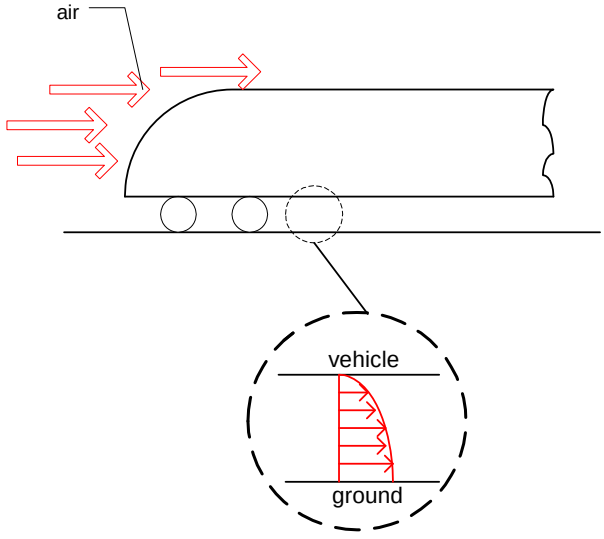

Fig. 3 Speed distribution at the inferior side of the vehicle body

In the wind tunnel there is, however, a permanent air cushion at the contact with the ground (between the floor and replica).

If this air cushion is quite extended, it may influence the pressure and the air flow values under the body.

In order to diminish the "air cushion effect", the following measures can be taken:

- minimizing the floor length of the wind tunnel;
- perfectly finishing the surfaces - the smoother the replica is, the smaller the air cushion limit is.

For example, the wind tunnels used by SNCF [4], have 10 m in length and the replica of the vehicle to be studied has 3 m (1:7 scale).

The roughness of the wooden or concrete floors has led, initially to some problems. The solution found was to suck out the air between the body and the floor (fig. 4).

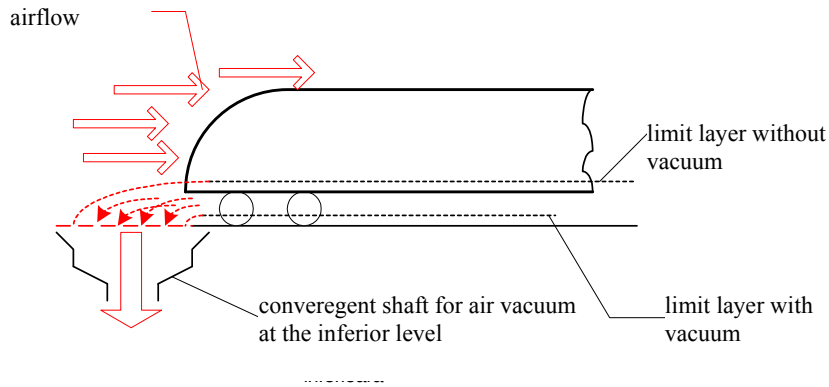

Fig. 4 Air-vacuum at the lower side of the replica

Another possible solution to simulate the real situation is the mobile floor – under the form of a conveyor belt (fig.5), which speed is equal with the one of the air flow.

This solution gives a more realistic simulation, by eliminating almost completely the permanent air cushion.

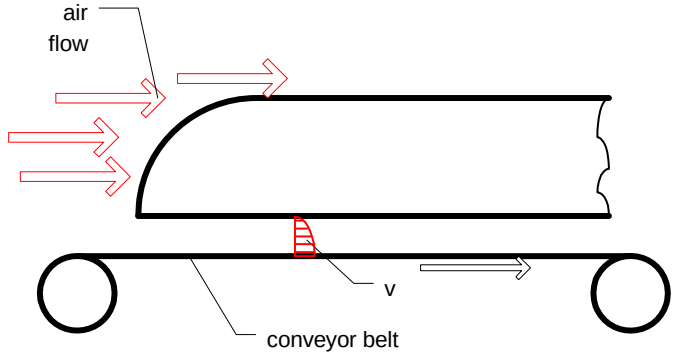

Fig.5 The mobile floor sol ution

The main factor influencing the aerodynamic drag of a ground vehicle resides in the complex term incorporated in the general equation that describes the total (mechanical and aerodynamic) drag:

$$R = r \cdot m \cdot g = \left[A + (k_w B_1 + B_2)V + k_t k_w k_y C_x S\rho \cdot \frac{1}{2} \cdot V^2 \pm i + r_c \right] mg \text{ [N]} \qquad (12)$$

The C_x coefficient can be measured with maximum accuracy in wind tunnels [7, 8], but correct enough approximations can be also achieved by launching the vehicle on a known slope, only when knowing the other mechanical resistances.

The influence of the wind can be expressed through two correction coefficients, k_w and k_y (both being functions of the speed of train and of the speed and wind direction).

The k_w coefficient expresses the relative velocity of the train compared to the one of the air (resulting from the speed of movement and from the speed of the wind). This applies, in the same way, to the B_1 term.

The k_y coefficient expresses the change of the penetration coefficient C_x in case of aerodynamic drag.

Another effect on the aerodynamic drag to motion resistance is determined by tunnels. The tunnel effect has been recently carefully studied, especially in the case of high-speed trains.

This effect can be expressed through a coefficient, noted still as k_t [6].

The influences of the gradients and curves are also to be taken into account in order to express the accurate value of the total drag.

When one has to deal with the calculus of the specific aerodynamic drag, the most important coefficient that must be taken into account is the frontal one. Its influence is best illustrated by the following equation:

$$C_x = \int_S C_p \frac{dS_x}{S_r} = \int_S \frac{p - \overline{p}}{\frac{1}{2}\overline{\rho} \cdot \overline{u}^2} \cdot \frac{dS_x}{S_r} = \frac{F_x}{\frac{1}{2}\rho \cdot \overline{u}^2 S_r} \tag{13}$$

C_x may be determined theoretically by integrating the pressure coefficient, C_p. In the equation above F_x – the total effective force to which the body is subjected to; $\overline{U}$ - the average fluid speed [m/s]; S_r – the reference surface [m^2]; ρ – the fluid density [kg/m^3].

3. THE PRACTICAL CASE STUDY

In order to illustrate the influence of the aerodynamic performance of a ground vehicle we have chosen the case of a railway traction vehicle.

The test was performed at INCAS subsonic wind tunnel, which has the following technical specifications: closed circuit, wind tunnel section 2,5 m x 2 m; air speed: 7-110 m/s; longitudinal yaw angle: ±45º; lateral yaw angle: -140º up to 216º; Reynolds number: 1,5-2,5x10^6; contraction surface ratio k=10; turbulence factor: 1,11.

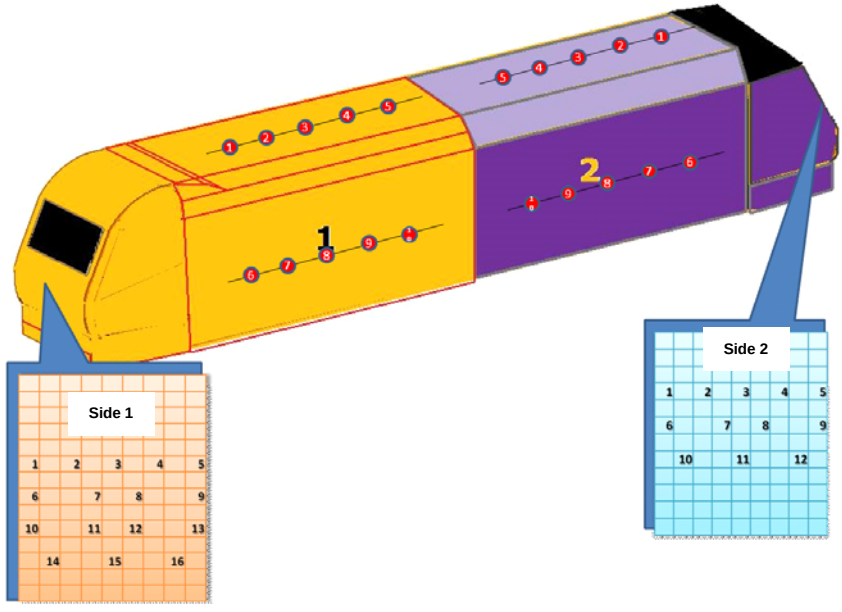

Fig.6 Pressure gauge installation.

The replica was build using polystyrene foam and had two different shapes at the ends. One had a poor aerodynamic shape and the other had a streamlined aerodynamic shape.

As far as the modelling theory allows it, we preferred to use the special replica solution, which has an exact geometric scale (non standardized, because the influence of such particularities of the real model do not influence the behaviour of the scale replica).

The vehicle studied has a top speed of 100-120 km/h (depending on its built class). In order to cover the intermediate speed range, we performed the test at 30 m/s (108 km/h).

The pressure gauges were installed as shown in figures 6-8.

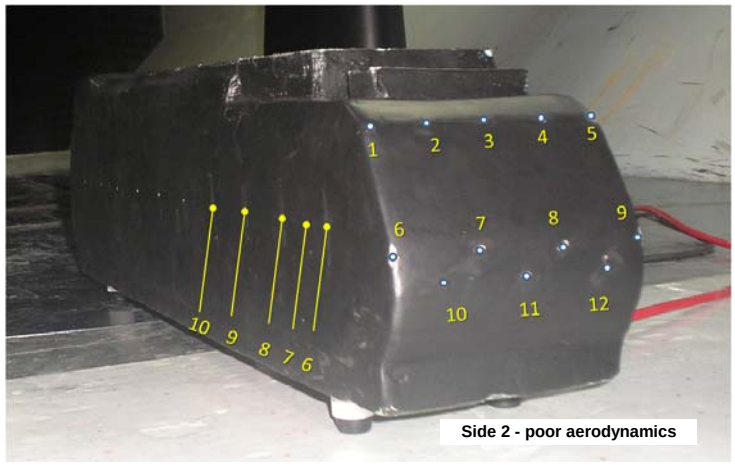

Fig.7. Pressure gauge installation on side 2.

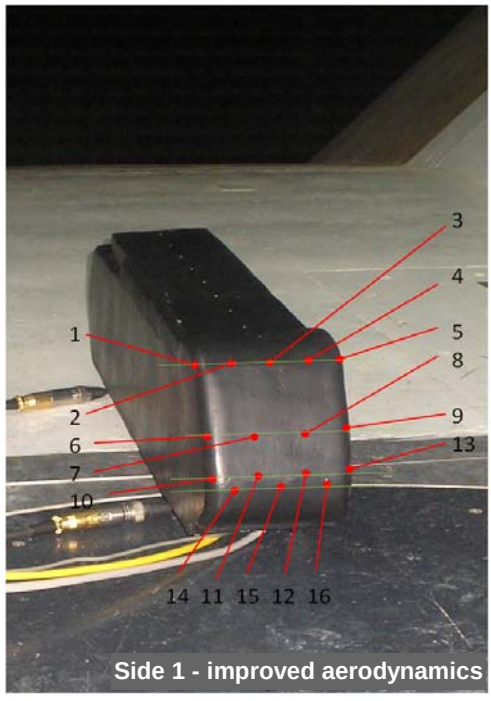

Fig.8. Pressure gauge installation on side 1.

The measurements of the pressures at each gauge mounted on the experimental replica were done through two electronic pressure scanners *Scanivalve* type, which can carry up to 16 simultaneous pneumatic connections.

The following results were obtained: for side 1 see Table 1, and for side 2 see Table 2.

Table 1

pressure gauge	p [psi]	p [kPa]	p_0 [psi]	p_0 [kPa]	C_p
P1	-0.09254	-0.63803	-0.00781	-0.05385	-1.05973514
P2	-0.07125	-0.49122	-0.00733	-0.05056	-0.799391606
P3	-0.10078	-0.69487	-0.0083	-0.05721	-1.156755788
P4	-0.06997	-0.48241	-0.00948	-0.06533	-0.756603462
P5	-0.1176	-0.81082	-0.0078	-0.05381	-1.373260548
P6	-0.12687	-0.87475	-0.00828	-0.05706	-1.483339022
P7	0.023728	0.163599	-0.02371	-0.16345	0.593293083
P8	0.040138	0.276742	-0.00909	-0.06267	0.615719024
P9	-0.16026	-1.10495	-0.00933	-0.06432	-1.887756405
P10	-0.06884	-0.47463	-0.00821	-0.05657	-0.758379526
P11	0.057039	0.39327	-0.00918	-0.06329	0.828221385
P12	0.060004	0.413713	-0.00823	-0.05672	0.853398975
P13	-0.12109	-0.83486	-0.00931	-0.06417	-1.39807542
P14	0.050707	0.349612	-0.00943	-0.065	0.752138285
P15	0.064981	0.448028	-0.00867	-0.05977	0.921177097
P16	0.055811	0.384803	-0.00922	-0.06355	0.813337464
P17	-0.07757	-0.53481	-0.00894	-0.06166	-0.858326928
P18	-0.01813	-0.12497	-0.00915	-0.06311	-0.112217256
P19	-0.0156	-0.10754	-0.00934	-0.0644	-0.078259404
P20	-0.0167	-0.11513	-0.0087	-0.06001	-0.099984925
P21	-0.01394	-0.09609	-0.00926	-0.06385	-0.05849756
P22	-0.02669	-0.18405	-0.00982	-0.06769	-0.211089014
P23	-0.01641	-0.11314	-0.00883	-0.06087	-0.094819329
P24	-0.01948	-0.13433	-0.00883	-0.06089	-0.133217342
P25	-0.00946	-0.06524	-0.00946	-0.06524	0
P26	-0.01315	-0.09067	-0.00935	-0.06449	-0.047490963
P27	-0.01539	-0.1061	-0.00813	-0.05606	-0.0907669
P28	-0.01726	-0.119	-0.00922	-0.06355	-0.100597792
P29	-0.01851	-0.1276	-0.00991	-0.06829	-0.107589483
P30	-0.01821	-0.12558	-0.00963	-0.06641	-0.107339333
P31	-0.01661	-0.11449	-0.0086	-0.05928	-0.10016003
P32	-0.01394	-0.09609	-0.00658	-0.0454	-0.09196762

Table 2

pressure gauge	p [psi]	p [kPa]	p_0 [psi]	p_0 [kPa]	Cp
P1	-0.0549	-0.37855	-0.00781	-0.05385	-0.58902
P2	-0.04361	-0.30065	-0.00733	-0.05056	-0.45368
P3	-0.03764	-0.25954	-0.0083	-0.05721	-0.36703
P4	-0.03549	-0.24471	-0.00948	-0.06533	-0.3254
P5	-0.06009	-0.41432	-0.0078	-0.05381	-0.65399
P6	-0.06191	-0.42687	-0.00828	-0.05706	-0.67085
P7	0.039621	0.273177	-0.02371	-0.16345	0.792075
P8	0.055257	0.380984	-0.00909	-0.06267	0.80482
P9	-0.0809	-0.55781	-0.00933	-0.06432	-0.89521
P10	0.054275	0.374213	-0.00821	-0.05657	0.781468
P11	0.063964	0.441016	-0.00918	-0.06329	0.914836
P12	0.056524	0.389719	-0.00823	-0.05672	0.809873
P13	-0.01203	-0.08296	-0.00931	-0.06417	-0.0341
P14	-0.01239	-0.08542	-0.00943	-0.065	-0.03703
P15	-0.01148	-0.07912	-0.00867	-0.05977	-0.0351
P16	-0.0117	-0.08068	-0.00922	-0.06355	-0.03108
P17	-0.07089	-0.48874	-0.00894	-0.06166	-0.77475
P18	-0.0427	-0.29441	-0.00915	-0.06311	-0.41959
P19	-0.01859	-0.12818	-0.00934	-0.0644	-0.11569
P20	-0.01439	-0.09924	-0.0087	-0.06001	-0.07116
P21	-0.01656	-0.11416	-0.00926	-0.06385	-0.09127
P22	-0.06243	-0.43045	-0.00982	-0.06769	-0.65807
P23	-0.04665	-0.32161	-0.00883	-0.06087	-0.47298
P24	-0.0103	-0.07104	-0.00883	-0.06089	-0.01841
P25	-0.00853	-0.05884	-0.00946	-0.06524	0.011607
P26	-0.01371	-0.0945	-0.00935	-0.06449	-0.05443
P27	-0.0125	-0.08621	-0.00813	-0.05606	-0.05468
P28	-0.01337	-0.09221	-0.00922	-0.06355	-0.05199
P29	-0.01321	-0.09106	-0.00991	-0.06829	-0.0413
P30	-0.01226	-0.08452	-0.00963	-0.06641	-0.03286
P31	-0.01096	-0.07556	-0.0086	-0.05928	-0.02953
P32	-0.00898	-0.0619	-0.00658	-0.0454	-0.02994

By analyzing the results and the graphic representations one can observe that the aerodynamically streamlined shape of the vehicle influences the air flow

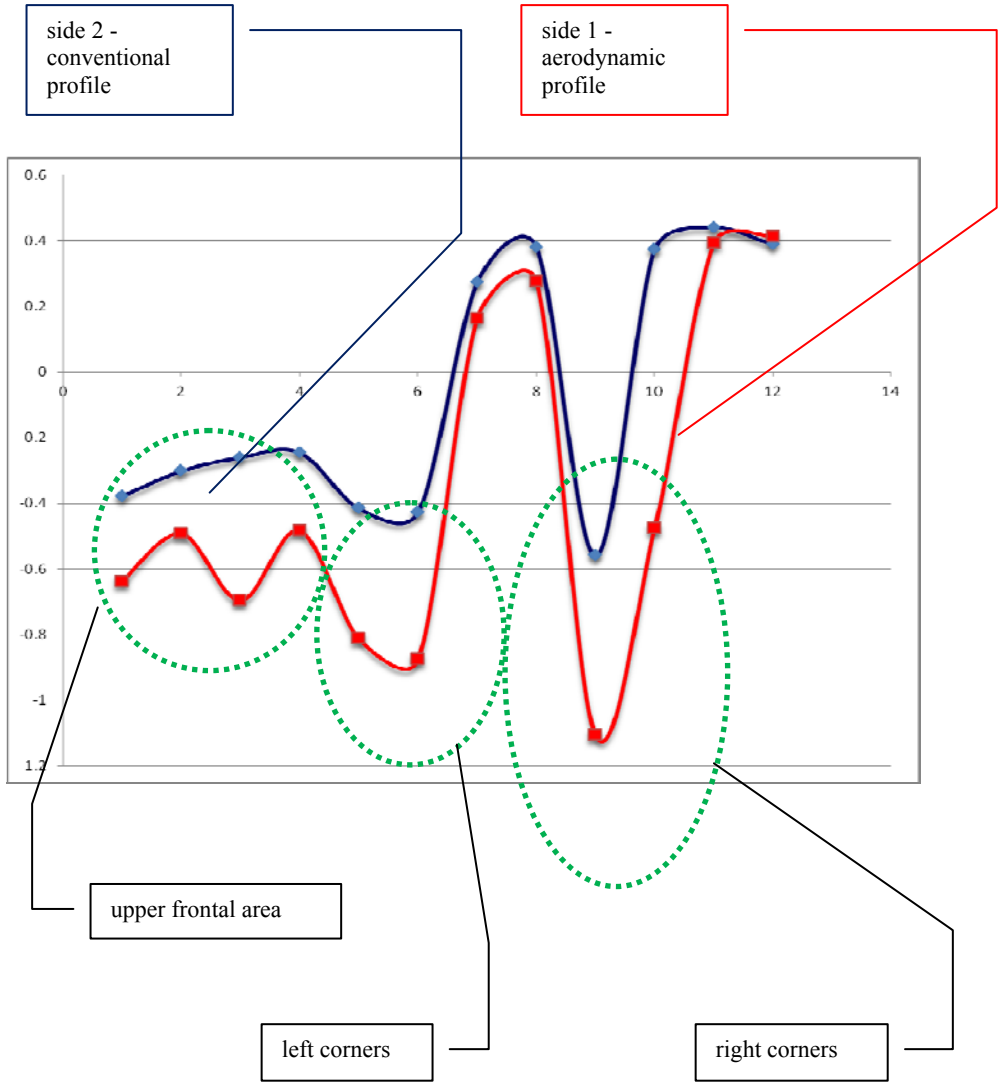

Fig. 9 Pressure distributions [kPa] on frontal surfaces of the model

4. CONCLUSION

The present work has illustrated the importance of aerodynamic design of the railway vehicles, as their performances are influenced by the aerodynamic drag.

Taking as a starting point a real body shape and proposing a new and improved one we have demonstrated that the size and quality of the frontal and lateral surfaces are, indeed, influencing the aerodynamic drag and thus, the energetic consumption.

The experiment also confirmed the computer simulations and analysis which concluded that even at inferior (subsonic) top speeds (commonly used in rail and automotive applications) improved aerodynamics may, indeed, influence the dynamic and traction performances.

REFERENCES

[1] S. Askey, T. Sheridan, *Safety of high speed ground transportation systems*, MIT, Cambridge, MA, 1996.
[2] P. Lukaszewicz, *Running resistance and energy consumption of ore trains in Sweden*, Proceedings of the Institution of Mechanical Engineers, Part F: *Journal of Rail and Rapid Transit 223*, 189-197, 2009.
[3] S. Krajnvic, *Shape optimization of high-speed trains for improved aerodynamic performance*, Proceedings of the Institution of Mechanical Engineers, Part F: *Journal of Rail and Rapid Transit 223*, 439-452, 2009
[4] A. Willaime, *L'aérodynamisme au matériel et à la traction, Revue Générale des Chemins de Fer*, décembre 1995, pp.5.
[5] P. Lukaszewicz, *A simple method to determine train running resistance from full-scale measurements*, Proceedings of the Institution of Mechanical Engineers, Part F: *Journal of Rail and Rapid Transit 221*, 331-338, 2007.
[6] P. Lukaszewicz, *Running resistance – results and analysis of full-scale tests with passenger and freight trains in Sweden,* Proceedings of the Institution of Mechanical Engineers, Part F: *Journal of Rail and Rapid Transit 221*, 183 -193, 2007.
[7] A. Radosavljevic, *Measurement of train traction characteristics*, Proceedings of the Institution of Mechanical Engineers, Part F: *Journal of Rail and Rapid Transit 220*, 283-291, 2006.
[8] S-W. Kim, H-B. Kwon , Y-G. Kim, T-W. Park, *Calculation of resistance to motion of a high-speed train using acceleration measurements in irregular coasting conditions*, Proceedings of the Institution of Mechanical Engineers, Part F: *Journal of Rail and Rapid Transit 220*, 2006, 449-459.